Clin. Lab. 2025;71:XXX-XXX

ORIGINAL ARTICLE

Identification of Endoplasmic Reticulum Stress-Related Gene Signature Reveals KRT8 as a Target in Ovarian Cancer

Xiaoyu Li [1, 3], Wulin Shan [1], Wenju Peng [3], Qi Zhu [1], Xu Huang [1, 3], Yao Chen [3], Zengying Wang [2], Bairong Xia [1, 3]

[1] *The First Affiliated Hospital of USTC, Division of Life Sciences and Medicine, University of Science and Technology of China, Hefei, Anhui, P. R. China*
[2] *Bengbu Medical College Bengbu, Anhui, P. R. China*
[3] *Department of Obstetrics and Gynecology, The First Affiliated Hospital of USTC, Division of Life Sciences and Medicine, University of Science and Technology of China, Anhui Provincial Cancer Hospital, Hefei, Anhui, China*

SUMMARY

Background: **Ovarian cancer (OC) is an invasive gynecological cancer with an overall 5-year survival rate of less than 45%. Endoplasmic reticulum (ER) stress plays a crucial role in regulating oncogenic events and immune-modulatory pathways, influencing malignant progression, antitumor immunity, and treatment response. However, the full scope of ER stress in ovarian cancer remains poorly understood and warrants further investigation.**
Methods: **RNA sequencing and clinical data were sourced from the Cancer Genome Atlas (TCGA) and Gene Expression Omnibus database (GEO). ER stress-related genes associated with ovarian tumor prognosis were identified, and an ER stress risk score model was developed using LASSO regression. We utilized this ER stress risk score to explore differences in immune cell infiltration. Furthermore, the biological role and expression of the risk gene KRT8 were validated through molecular biology experiments.**
Results: **We identified 573 genes related to ER stress that were differentially expressed genes (DEGs) between normal and tumor tissues. The ER stress-related risk signature (ERRS) constructed using the TCGA dataset was regarded as an independent and significant prognostic model for predicting cancer progression and instructing clinical decisions. Additionally, KRT8 was found to be overexpressed in ovarian cancer cells and tissues. Downregulation of KRT8 inhibited ovarian cancer cell proliferation and migration (in both SKOV3 and OVCAR8 cells) *in vitro*.**
Conclusions: **The ER stress-related gene model we developed can be utilized to assess the prognostic risk for OC patients. Importantly, KRT8 was identified as a key risk gene in ovarian cancer, promoting tumor progression, and holds potential as a novel therapeutic target.**
(Clin. Lab. 2025;71:xx-xx. DOI: 10.7754/Clin.Lab.2025.241216)

Correspondence:
Bairong Xia
The First Affiliated Hospital of USTC
Division of Life Sciences and Medicine
University of Science and Technology of China
Anhui Provincial Cancer Hospital
Hefei
Anhui, 230031
P. R. China
Email: xiabairong@ustc.edu.cn

Manuscript accepted March 5, 2025

KEYWORDS

ovarian cancer, endoplasmic reticulum stress, tumor immune microenvironment, KRT8

INTRODUCTION

Background

Ovarian cancer (OC) is the third most common gynecologic malignancy worldwide. According to the World Health Organization, the global incidence of OC is estimated to be 225,500 cases, and 140,200 patients will

succumb to this disease each year, making it the eighth most predominant cause of cancer-related death among women [1]. Most OC patients are at an advanced stage and lost the opportunity for surgery due to lack of effective screening tools [2]. Furthermore, emerging diagnosis and therapies for ovarian cancer, including molecular targeting agents and immunotherapies, have improved the prognosis of a subset of OC patients, but the response rate remains limited [3]. To improve survival in patients with this aggressive disease, the immunological state of the tumor microenvironment must be determined [4]. Additionally, refining predictive biomarkers and developing innovative treatments are crucial to identifying patients who will benefit from chemotherapy, targeted therapies, or immunotherapy, enabling more personalized treatment. Therefore, there is a pressing need to develop effective tools for predicting survival and identifying new targets for OC treatment.

To maintain ER homeostasis and ensure protein folding fidelity, the unfolded protein response (UPR), an adaptative mechanism, has emerged to improve the protein folding capacity of the ER and relieve the load of unfolded or misfolded proteins [5]. However, diverse stressors, including hypoxia, nutrient deprivation, low pH, reactive oxygen species (ROS) overproduction, high transcription and translation rates, drugs, and radiation, disturb the protein folding capacity of the ER and provoke a cellular state of "ER stress" [6]. As the ER connects directly to other organelles, including the mitochondria, nucleus, and cytoskeleton, ER stress can globally affect biological functions in cells. In malignant cells, sustained stressors in the tumor microenvironment (TME) induce persistent ER stress, which has been proven to drive tumor initiation, progression, and resistance to therapy [7].

Rationale and knowledge gap

Previous studies showed that elaiophylin-inducing ERS triggers paraptosis overcame drug resistance to platinum, taxane, or PARPi in OC [8]. In addition, ER-associated proteins including glucose-regulated protein (GRP78) are increased in EOC patients and can be used as predictors of survival [9]. Chen et al. established an ER stress-associated risk signature for pancreatic cancer patients and it can be used to guide clinical decision making in the immunotherapy and predict survival [10]. However, the predictive role of ERS in OC has not been fully elucidated.

Objective

This study aimed to analyze differential ERS-related genes between ovarian cancer tissues and normal tissues and explored the biological functions and pathways associated with these DEGs. The ER stress-related risk signature (ERRS) was constructed using differentially expressed genes (DEGs) to evaluate the prognosis of OC patients. Additionally, we performed an association analysis between these key genes and immune infiltration. Quantitative polymerase chain reaction (qPCR) and immunohistochemistry (IHC) revealed that KRT8 was upregulated and could regulate the migration and invasion of OC cells. The flow chart of this study can be seen in Figure S1. Our study established a model of ER stress-related genes for assessing the prognosis of OC and reveals KRT8 as a potential new therapeutic target.

MATERIALS AND METHODS

Data collection

The RNA-seq data for gene expression (count and FPKM value) and associated clinical information were obtained from The Cancer Genome Atlas (TCGA) (https://cancergenome.nih.gov/) and the Genotype-Tissue Expression (GTEx) database (http://xenabrowser.net/). The RNA-seq data included 515 patient samples, 427 tumor samples, and 88 normal tissue samples (Table S1). In addition, the GSE26712, GSE49997, GSE102073, and GSE140082 datasets were obtained from the Gene Expression Omnibus (GEO) database (http://www.ncbi.nlm.nih, gov/geo/) as a validation cohort to verify the predictive value of the risk model. A list of unfolded protein response-related genes was obtained from the HALLMARK and REACTOME gene sets of the Molecular Signatures Database. Then, 1,176 ER stress-related genes were extracted from GeneCards for subsequent analysis, and genes with a relevance score > 5 were selected.

Multiomics analysis of ER stress-related genes

We adjusted for batch effects in the expression data and determined differentially expressed genes (DEGs) related to ER stress in ovarian cancer and normal tissues by the R software "DESeq2" package ($|\log_2 (FC)| = 0.5$ and $p < 0.05$). A heatmap and volcano plot reflecting the difference in the expression of each differentially expressed ER stress-related gene between normal and tumor tissues were generated with the "pheatmap" and "ggplot2" packages in R. Principal component analysis (PCA) conducted with the "ggbiplot" package was used to verify the accuracy of the classifications. We downloaded the mutation and copy number variation (CNV) data of ovarian cancer patients and constructed waterfall plots with the "maftools" package. Kaplan-Meier curve analysis via the "survival" package was used to compare the survival possibility between the mutation group and the wild-type group.

Construction and verification of the ER stress-related risk signature (ERRS)

In the training cohort, univariate Cox regression analysis was conducted using the "survival" package in R to screen for ER stress-related genes with significant prognostic value ($p < 0.05$). Kaplan-Meier curve analysis via the "survival" and "survminer" packages was used to compare the survival possibility between patients with high and low expression of the differentially expressed

ER stress-related genes. The ERRS for predicting the prognosis of OC patients was constructed through Cox and least absolute shrinkage and selection operator (LASSO) regression analyses by using the "glmnet" software package in the R language. According to the penalty parameter (λ) determined by "cv.glmnet", we reconstructed a model and screened ER-related genes.

Risk score = $\sum_{i=1}^{N}(Coef_i \times Exp_i)$

Expi is the expression value of the ER stress-related genes, and Coefi is the corresponding regression coefficient calculated by Cox analysis. The TCGA data were used as the training cohort, and the GSE26712, GSE49997, GSE102073, and GSE140082 cohorts were used as the validation cohorts. Patients in the two databases were divided into high- and low-risk groups according to the median risk score for follow-up evaluation.

Survival analysis

We used the "ggsurvival" package in R to construct a Kaplan-Meier survival curve to assess the difference in survival between the high- and low-risk groups. The receiver operating characteristic (ROC) curve and the area under the curve (AUC) were used to assess the ability of the genetic and clinical factors to predict survival at 1, 3, and 5 years. Additionally, the "pheatmap" package in R was used to construct the risk map. In the survival analysis, p-values < 0.05 were considered to indicate statistical significance and were used for subsequent analysis.

Construction of the predictive nomogram

The nomogram shows the probability of clinical events through simple graphs of statistical prediction models to form a personalized prediction model. The risk score, stage, grade, neoplasm status, and age were combined to develop a nomogram using the "survival" and "regplot" packages in the R language. Calibration curves and receiver operating characteristic (ROC) curves were generated to evaluate the ability of the nomogram to predict the one-, two-, and three-year survival probability of ovarian cancer patients. The bootstrap resampling method was used to evaluate the discrimination ability of the nomogram.

Analysis of the association between the ERRS and immunity in OC patients

The analytical method CIBERSORT (https://cibersort.stanford.edu/) can be used to characterize the cell composition of a mixed cell population. We applied CIBERSORT to estimate the relative abundance of TIME-infiltrating immune cells between the high- and low-risk score groups. To further investigate the potential association between TIME-related ER stress and clinical immunotherapy efficacy, we analyzed the expression of immune checkpoint genes in the high- and low-risk score groups. Immune checkpoint gene information was acquired from previous literature [11]. A boxplot was generated to compare the levels of immune cell infiltration, immune scores, and differentially expressed immune checkpoint genes.

Cell culture and specimen collection

A human normal ovarian epithelial cell line (IOSE-80) and ovarian cancer cell lines (HOC-7, A2780, SKOV3, OVCAR8, HEYA8, and CAOV3) were purchased from EK-Bioscience (Shanghai, China). HOC-7, A2780 OVCAR8 cells were maintained in RPMI 1640 (Hyclone, Cytiva, UT, USA) supplemented with 10% fetal bovine serum (FBS) at 5% CO2 at 37°C. SKOV3 was cultured in McCoy's 5a (Hyclone, Cytiva, UT, USA) medium and 10% FBS. HEYA8 and CAOV3 were cultured in DMEM medium (Hyclone, Cytiva, UT, USA). SiRNA against KRT8 was provided by RIBORIO (Guangzhou, China). Si-NC was used as a negative control. Transfection was performed with CP Transfection Kit (RIBORIO, Guangzhou, China) according to the manufacturer's instructions. The siRNA targeting sequences against KRT8 in this study were as follows:
si#1: GTGGAGAGCTGGCCATTAA,
si#2: TCACCGCAGTTACGGTCAA,
si#3 CTCGAAGCAACATGGACAA.

Immunohistochemistry

All tissues were frozen in liquid nitrogen within 30 minutes after resection and stored at -80°C. Tumor tissues were fixed in 10% formalin, embedded after dehydration. Slides were incubated with KRT8 antibody (1:500, proteintech, Wuhan, China). This study was approved by the Medical Ethics Committee of the First Affiliated Hospital of the University of Science and Technology of China.

Western blot

RIPA buffer (Beyotime, Shanghai, China) was used for protein extraction. The protein concentration was measured using a BCA protein assay kit (Beyotime, Shanghai, China). Forty micrograms of protein were separated via SDS–PAGE and transferred onto PVDF membranes, which were subsequently blocked with 5% nonfat milk and incubated with relevant primary antibodies at 4°C overnight. Horseradish peroxidase-conjugated secondary antibodies were used to detect the primary antibodies. An enhanced chemiluminescence (ECL) detection system (Thermo Scientific, Waltham, MA, USA) was used to image the protein bands, and a semiquantitative analysis was conducted using ImageJ software. The primary antibodies used were those against GAPDH (1:10,000, ZSGB-BIO, Beijing, China).

Total RNA extraction and quantitative real-time PCR

Total RNA was extracted from cells or plasma using TRIZOL reagent (Invitrogen, Waltham, MA, USA). The RNA was reverse-transcribed into cDNA using a PrimeScript RT Reagent Kit (Beyotime, Shanghai, China). qPCR was performed using SYBR Green qPCR

Master Mix (Beyotime, Shanghai, China) on a ftc-3000p PCR instrument (fungyn biotechinc, Canada). cDNA was synthesized from total RNA (0.5 μg) at 48°C for 30 minutes and at 95°C for 10 minutes. cDNA (1 μg) was subjected to polymerase chain reaction (PCR) for 45 cycles of 94°C for 45 seconds, 56°C for 30 seconds, and 72°C for 30 seconds. The primers used for quantitative reverse transcription-PCR are summarized in Table 1. The data were analyzed using the 2-ΔΔCT method.

Cell viability assay

SKOV3 and OVCAR8 cells were seeded on a 96-well plate at a density of 2×10^3 cells/well. Cell viability was measured using a Cell Counting Kit (CCK-8) (BestBio, Shanghai, China) following the manufacturer's instructions. Cell viability was determined at 450 nm using a microplate reader (TECAN Group Ltd, Switzerland).

Colony formation assay

A colony formation assay was used to evaluate the clonogenic ability of the ovarian cancer cells. A single-cell suspension of cells was trypsinized at a density of 1×10^3 and was seeded on 6-well plates. Afterward, the cells were maintained in RIPM 1640 supplemented with 10% FBS (Gibco) for approximately 2 weeks. The visible colonies were fixed in 4% paraformaldehyde for 4 hours at 37°C and stained with 0.5% crystal violet (Beyotime, China) for 2 hours at 37°C. The colonies were counted under a light microscope (Olympus Corp).

Wound healing assay

Cell migration was detected by a wound healing assay as previously described. Cells were seeded on six-well plates. Pipette tips were used to create a clean cross on the well, and the cell debris was removed with PBS. Then, the solution was added, and the cells were cultured for 48 hours. The scratch images were observed by a microscope at × 40 magnification. The healing area was calculated by ImageJ analysis software.

Transwell assays

OVCAR8 and SKOV3 cells suspended in 200 μL of serum-free medium were seeded in transwell chambers. When appropriate cells were filtered to the bottom of the chamber, the cells were fixed with 4% paraformaldehyde and stained with crystal violet. Five random fields per group were photographed under an optical microscope, and the number of cells was counted.

Statistical analysis

All the data were processed in the R programming environment (version 4.0.3) and GraphPad Prism (version 9.0). The present study conducted statistical analyses, and Wilcoxon signed-rank tests were used to detect differences in immune cells and immune checkpoint molecules between the high- and low-risk populations. $p < 0.05$ was considered to indicate statistical significance.

RESULTS

Dysregulated expression of ER stress-related genes in ovarian cancer

First, we acquired the TCGA (427 ovarian cancer) and the GTEx (88 normal tissues) cohorts to investigate the expression of ER-related genes. In addition, we downloaded the hallmark and REACTOME gene sets from the Molecular Signatures Database (MSigDB) and identified unfolded protein response (UPR)-related genes. We screened 1,176 genes with a relevance score > 5 that correlated with endoplasmic reticulum stress and the unfolded protein response from the GeneCards database. In the pooled dataset, 573 ER-related genes were found to be significantly differentially expressed, including 357 upregulated and 216 downregulated genes (Table S2). The final DEGs were visualized by a volcano map (Figure 1A) and heatmap (Figure 1B). Copy number variation (CNV) is a genomic structural variation induced by a number of copies of a particular DNA segment [12]. The CNV signature is closely related to gene mutations in high-grade serous ovarian cancer (HGSOC) and can be used to predict overall survival (OS) and the prognosis of patients during chemotherapy treatment [13]. Therefore, we acquired mutation data for ovarian cancer patients and performed waterfall mapping for ER-related gene mutations (Figure 1C). TP53 and TTN mutations were found in 66% and 42%, respectively. Missense and nonsense mutations account for the majority of TP53 mutations, while multihit and nonsense mutations often occur in TTN. Next, we analyzed CNVs in the patients. The results showed that MAP3K4 and PLG CNVs occurred in 3% of the ovarian cancer patients, and most of the CNVs were amplification and deletion mutations (Figure 1D).

ER genes screened by univariate Cox regression analysis

We identified 32 ER genes with significant prognostic value ($p < 0.05$) among the DEGs by univariate Cox regression analysis (Table S3). The samples were divided into a high-expression group and a low-expression group according to the expression of the ER genes. Furthermore, we evaluated the correlations between ER stress-related genes and patient prognosis in the TCGA cohort. Kaplan-Meier survival analysis revealed that survival probability was significantly different in the high- or low-gene (TRIB3, MAP2K6, CNR1, GUCY 2D, EZH2 and ANXA2) expression groups (Figure S2). The survival probability in the group with low MAP 2K6 (HR = 0.741) or GUCY2D (HR = 0.657) expression was much lower than that in the group with high MAP2K6 expression, while patients with low TRIB3, CNR1, EZH2, and ANX2 expression tended to have a better prognosis. In addition, the expression of the six genes was also assessed. The expression levels of TRIB3, MAP2K6, GUCY2D, EZH2, and ANXA2 in ovarian cancer tissues were much lower than those in adjacent tissues. Conversely, CNR1 expression was

Table 1. Overview of primers in this study.

Gene	Forward primer sequence (5′-3′)	Reverse primer sequence (5′-3′)
CEBPG	AATACGACAGCAGATGGCGA	GGGTCTTTGAGTCATGGAAATG
NSDHL	GTGGGAAGGCATTTCACATCA	TAGCAGGAGGGCCAGGTAGT
PPP1R11	TACTTCCTAGACTTTGATTTCTCCG	GTGGTGGTATGGATTTGACTGAT
KRT8	TTGTGAAGAAGATCGAGACACGT	GTTCCCAGTGCTACCCTGCAT

Table 2. Induction of the six differentially expressed ERS-related genes with prognosis value in ovarian cancer (OC).

Gene	Gene name	Functions in OC	Reference
EZH2	enhancer of zeste 2 polycomb repressive complex 2 subunit	EZH2 upregulates IDH2 transcription to enhance TCA cycle activity, promoting metabolic reprogramming and facilitating ovarian cancer growth. It promotes cell proliferation and invasion, inhibits cell apoptosis, and enhances angiogenesis.	[32] [33]
KRT8	keratin 8	It regulates FAS-induced cell apoptosis in human ovarian granulosa cell tumors. It is related to stress states caused by oxidative imbalance and pro-inflammatory lipid signaling	[34] [35]
NSDHL	NAD(P) dependent steroid dehydrogenase-like	none	none
POLR2L	RNA polymerase II, I, and III subunit L	none	none
PPP1R11	protein phosphatase 1 regulatory inhibitor subunit 11	none	none
TRIB3	tribbles pseudokinase 3	it activates the MEK-ERK signaling pathway to promote tumor progression	[36]

higher in tumor tissues (Figure S2).

Establishing and evaluating the ER stress risk signature

Based on the results of univariate regression analysis, eight ER stress-related genes, GUCY2D, NPC2, CDK5, ANXA2, TRIB3, PML, TGM5, and EZH2, were used to construct a forest plot (Figure 2A). A total of 32 ER stress-related genes were used to construct a LASSO regression model, and the penalty parameter (λ) value of the training cohort was seven, as determined by "cv. glmnet" (Figure 2B). Finally, seven ER stress-related genes were used to construct the prognostic model. The risk score was calculated as (0.293*CEBPG exp) + (0.463*EZH2 exp) + (0.274*KRT8 exp) + (0.299*NSDHL exp) - (0.263*POLR2L exp) + (0.304*PPP1R11 exp) + (0.331*TRIB3 exp). Induction of the six differentially expressed ERS-related genes with prognosis in ovarian cancer OC were summarized in Table 2. Patients in the training cohort and testing cohort were separated into high- and low-risk groups according to the median risk score (median (fp) = 1.026694). Furthermore, the expression of ER-related genes was significantly different between the high- and low-risk score groups ($p < 0.01$; Figure 4G), as indicated by the heatmap (Figure 2C). Finally, a receiver operating characteristic (ROC) curve was used to evaluate the predictive role of risk scores on survival, and the area under the curve (AUC) values for 1-, 3-, and 5-year survival prediction for patients with an ERRS were 0.6045, 0.6288, and 0.6460, respectively (Figure 3D). These results showed that the prognostic model based on these ER-related genes has potential value in the prediction of ovarian cancer prognosis. This finding was further validated in the testing cohort. With respect to the GSE26712 dataset, the area under the curve (AUC) values for 1, 3, and 5 years were 0.5723, 0.5914, and 0.6297, respectively (Figure S3). Kaplan-Meier analysis revealed that survival probability was significantly different between the high- and low-risk score groups ($p < 0.01$). With increasing risk score, the survival probability of patients in the testing cohort gradually decreased (Figure S3). Furthermore, in the GSE102073 dataset, the area under the curve (AUC) values for 1-, 3-, and 5-year survival were 0.6248, 0.6429, and 0.6276, respectively, and there was a notable difference in survival probability between the two risk groups (Figure S3).

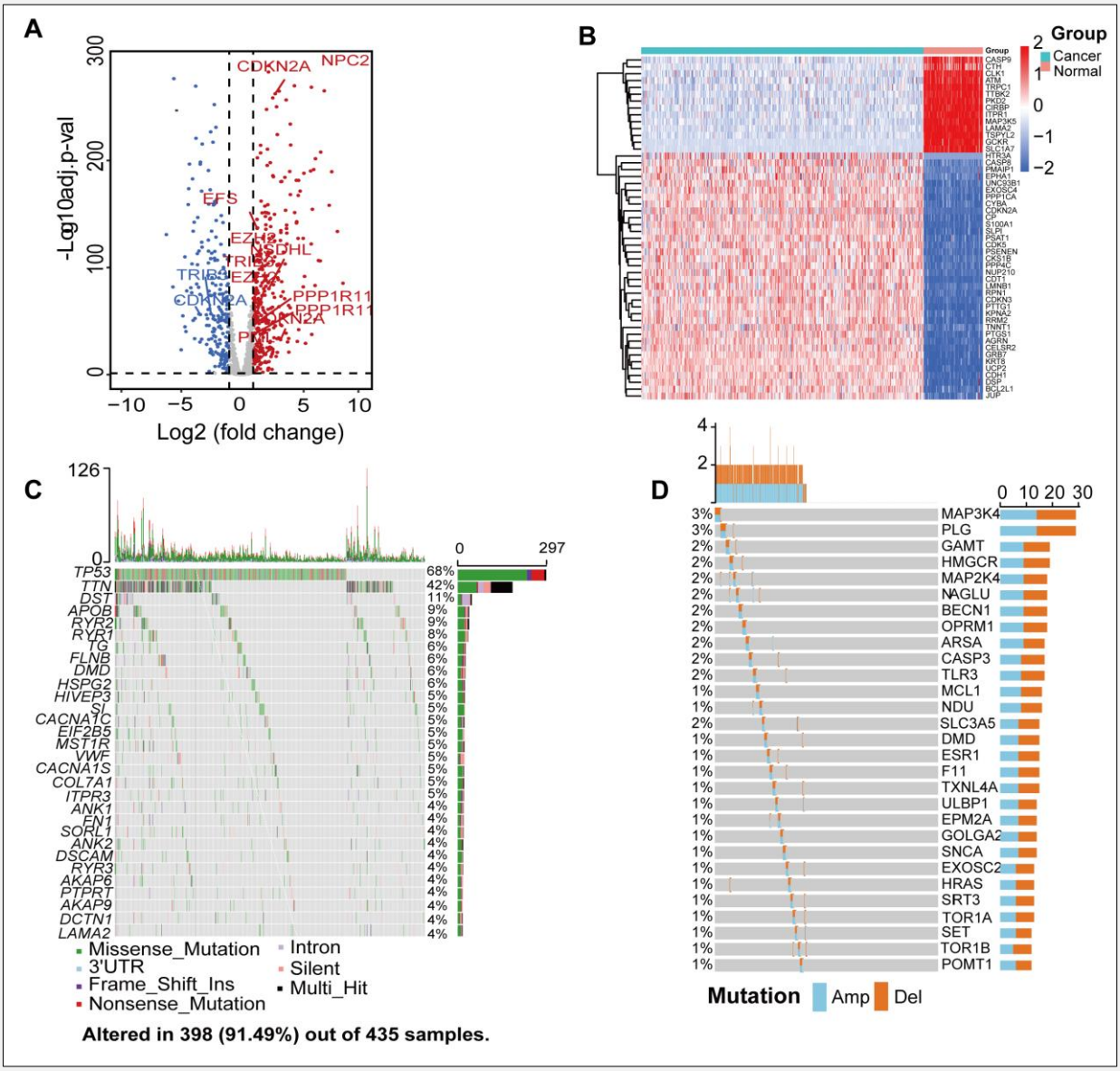

Figure 1. Identification of differently expressed ER-related genes between OC and normal samples.

A - Volcano plot of differentially expressed ER-related genes. The x-axis represents log_2Foldchange, and the y-axis represents -log_{10}padj. B – Heatmap of differentially expressed ER-related genes. C - Genomic-level variations and the impact of mutations on prognosis in ER-related genes. D - Waterfall plot of mutations in ER-related genes.

Relationships between the ERRS score and clinical characteristics in OC patients

To further integrate clinical information to achieve multivariate survival analysis, we collected all the clinical information of ovarian cancer patients in the TCGA and GEO databases (Table S4). Patients with high or low risk scores were divided into different clinical factors according to age (< 60 and > 60), stage (III and IV), and neoplasm status (yes and no) (Figure S4). The results showed that patients with high-risk scores had a notably lower survival probability than did those with low-risk scores in every subgroup ($p < 0.05$). In addition, by combining clinical factors, changes in the ERRS score during the development of cancer were analyzed. As shown in the boxplots (Figure S4), we calculated risk scores in different subgroups according to age, histolo-

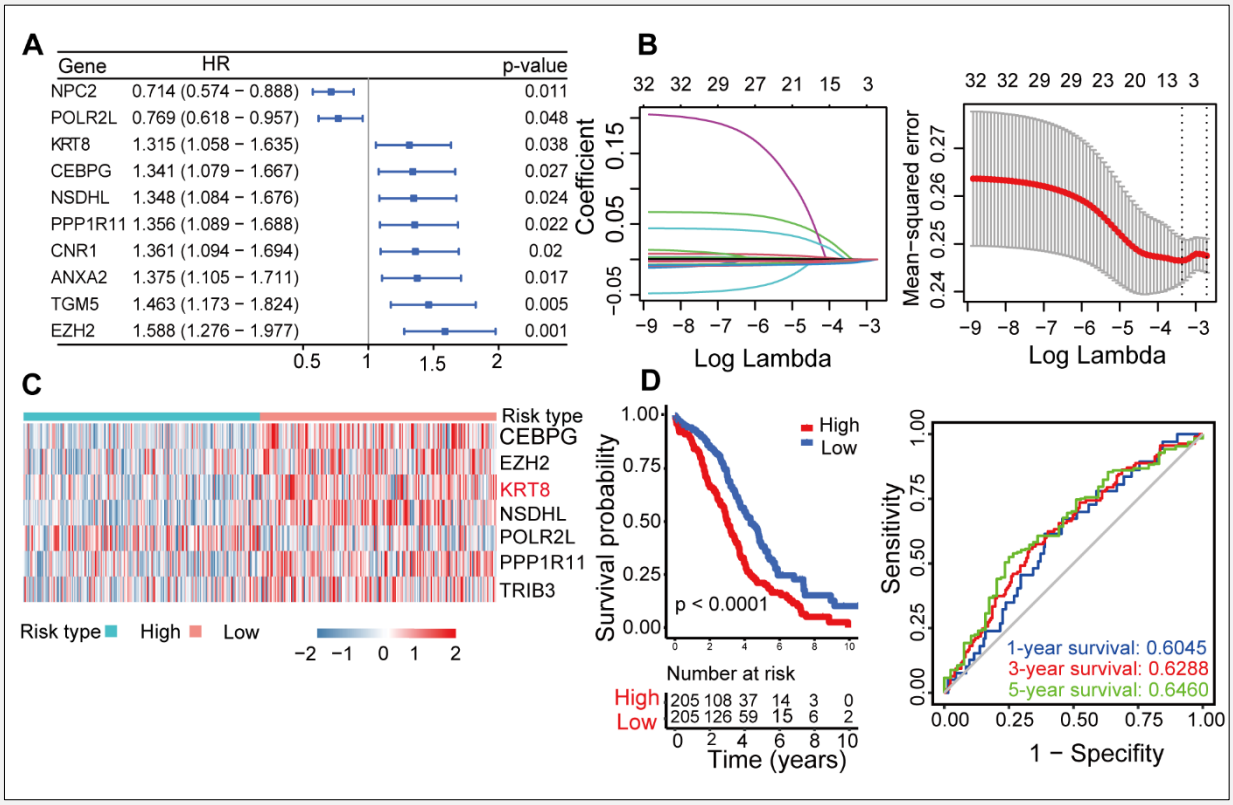

Figure 2. Construction of machine learning-based endoplasmic reticulum stress risk scoring model (ERRS) and prognostic performance analysis.

A - The forest plot of univariate analysis. B - Lasso regression model and optimal λ value. C - Expression levels of ER-related genes in high and low-risk groups of ovarian cancer. D - Kaplan-Meier survival curves for high and low-risk groups and prognostic model for 1-, 3-, and 5-year survival rates.

gic grade, lymphatic invasion, immune subtype, and stage. In the training cohort, the risk scores for these clinical characteristics were not significantly different between the high- and low-risk score groups (Figure S4). However, in the test cohort, the risk score for the immune type was notably different ($p < 0.01$) from that for other subtypes, such as the mesenchymal type. Furthermore, patients aged > 60 years had a greater risk score than those aged <60 years ($p < 0.05$). These analyses showed that ERRS score is closely associated with clinical characteristics.

Independent prognostic value of the ERRS

In addition to the ER stress risk score, clinical factors such as age, histologic grade, stage, and lymphatic invasion are also prognostic factors for ovarian cancer. Thus, to determine whether the ERRS is an independent predictive model that can improve the prediction of the prognosis of ovarian cancer patients, we used a training cohort and testing cohort to perform multivariate Cox regression analysis. The results showed that the prognostic risk model was independent of clinical factors, including age, histologic grade, lymphatic invasion, and stage, in the training cohort (Figure 3A). In the testing cohort, the ERRS score was independent of age and stage (Figure 3A). Next, we established a nomogram to predict 1-, 2-, and 3-year survival probabilities in the TCGA dataset by integrating the ERRS score and clinical factors (Figure 3B). These signatures were assigned points according to their risk contribution to survival probability. To further evaluate the predictive efficacy of the risk score and clinical characteristics, we applied a multi-indicator ROC curve analysis, and the results showed that our risk model (AUC = 0.641) was superior to age (AUC = 0.568), grade (AUC = 0.517), lymphatic invasion (AUC = 0.5), and stage (AUC = 0.528; Figure 3C). The calibration curves showed a remarkable consensus between the actual and nomogram-predicted sur-

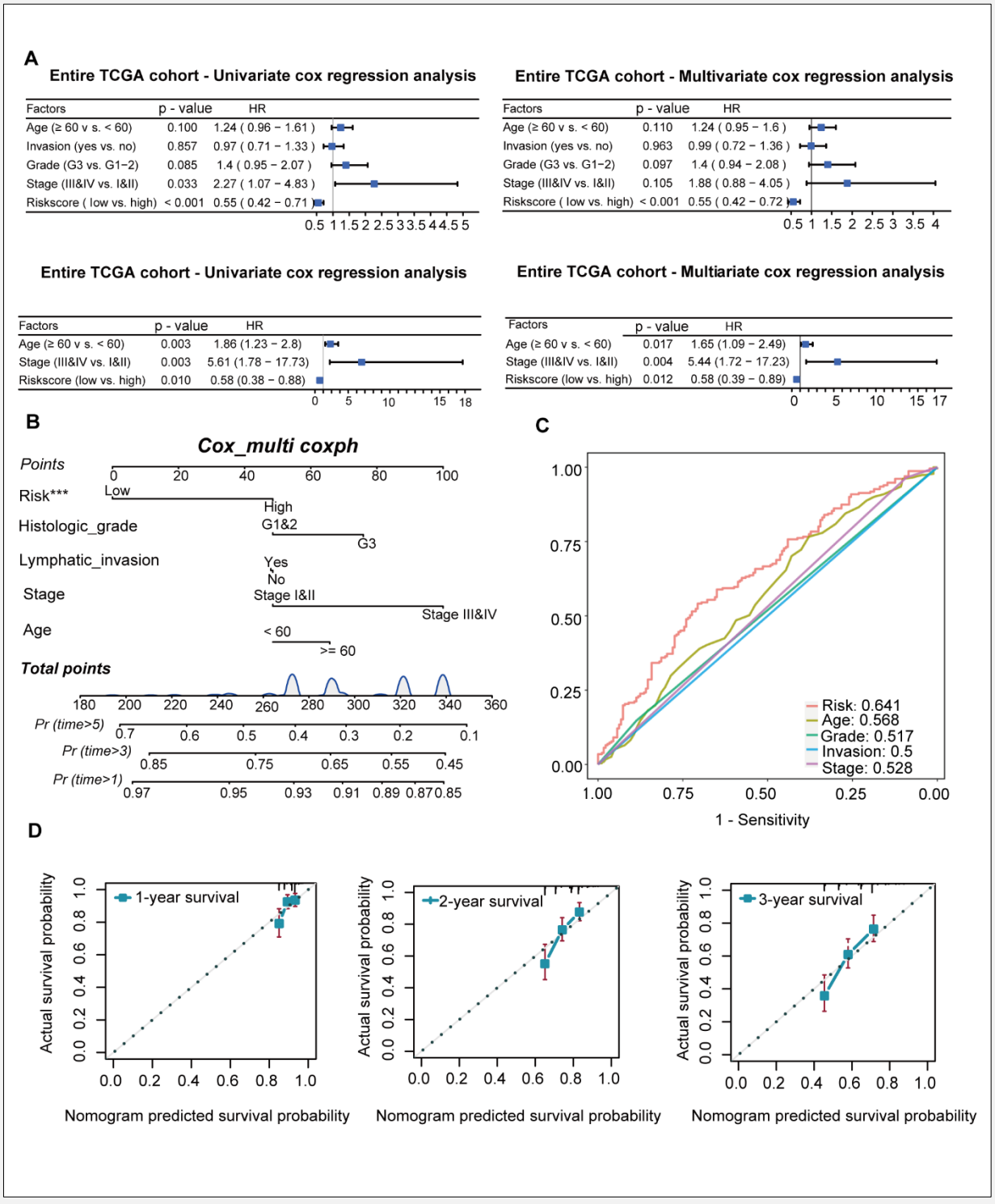

Figure 3. Verification that endoplasmic reticulum stress risk scores are an independent prognostic factor for cancer.

A - Univariate and multivariate Cox regression analysis of risk score and clinical factors in the training cohorts. Univariate and multivariate Cox regression analysis of risk score and clinical factors in the validation cohorts. B - Nomogram model based on risk model and clinical features, ** - p < 0.01, * - p < 0.001. C - Predictive efficacy of the nomogram compared with clinical factors through ROC curves. D - Calibration plots showing the association of the predicted 1-, 3-, and 5-year OS with actual survival duration.**

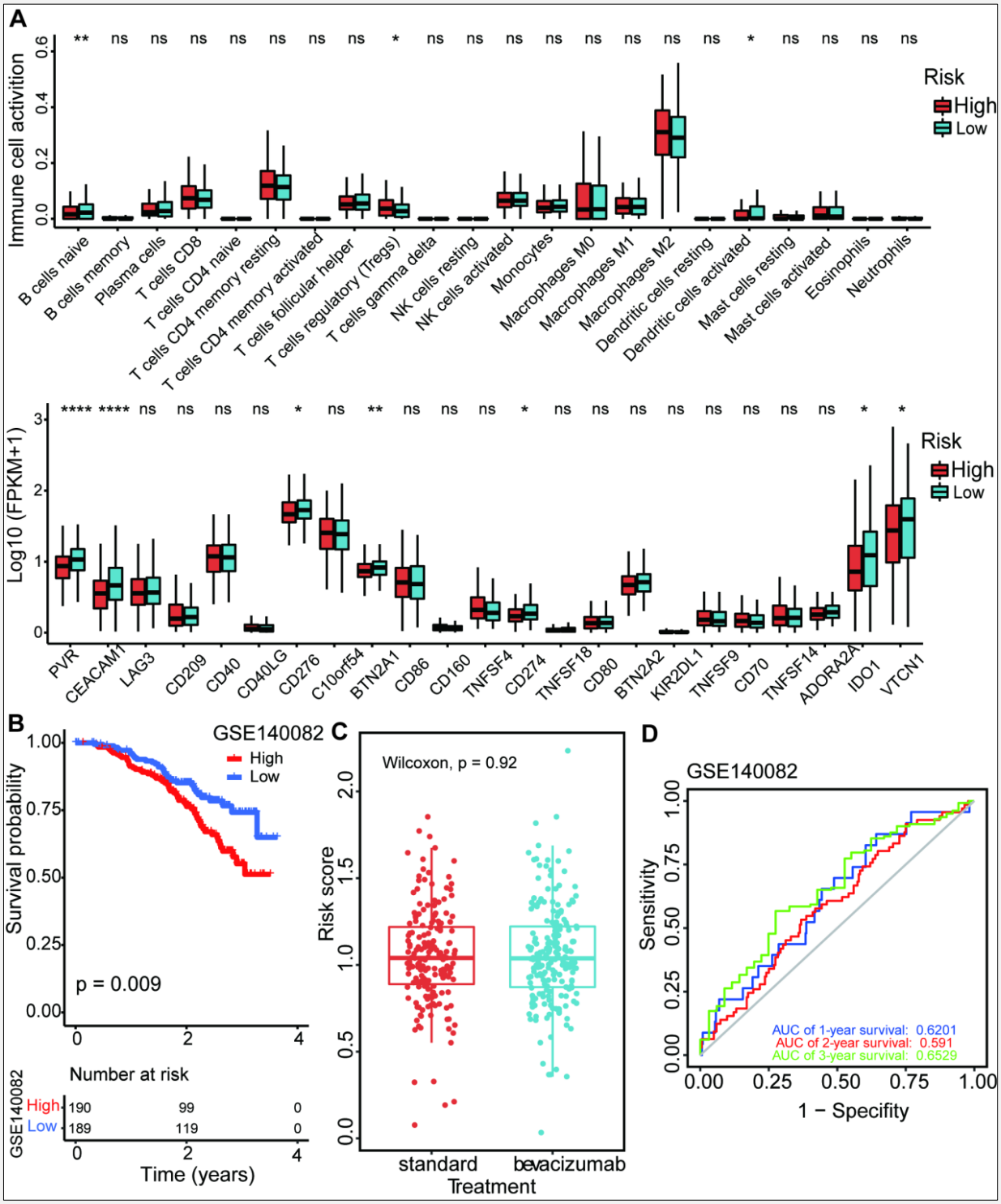

Figure 4. Immune landscape analysis and prediction treatment efficacy of ERRS in OC.

A - Differences in cell infiltration proportions between high and low-risk groups of ER-related genes (* - p < 0.05, ** - p < 0.01). Differences in expression of immune checkpoint markers between high and low-risk groups of ER-related genes (** - p < 0.0001, ** - p < 0.01, * - p < 0.05). B - D - Comparation of risk scores between the standard group and the bevacizumab treatment group.**

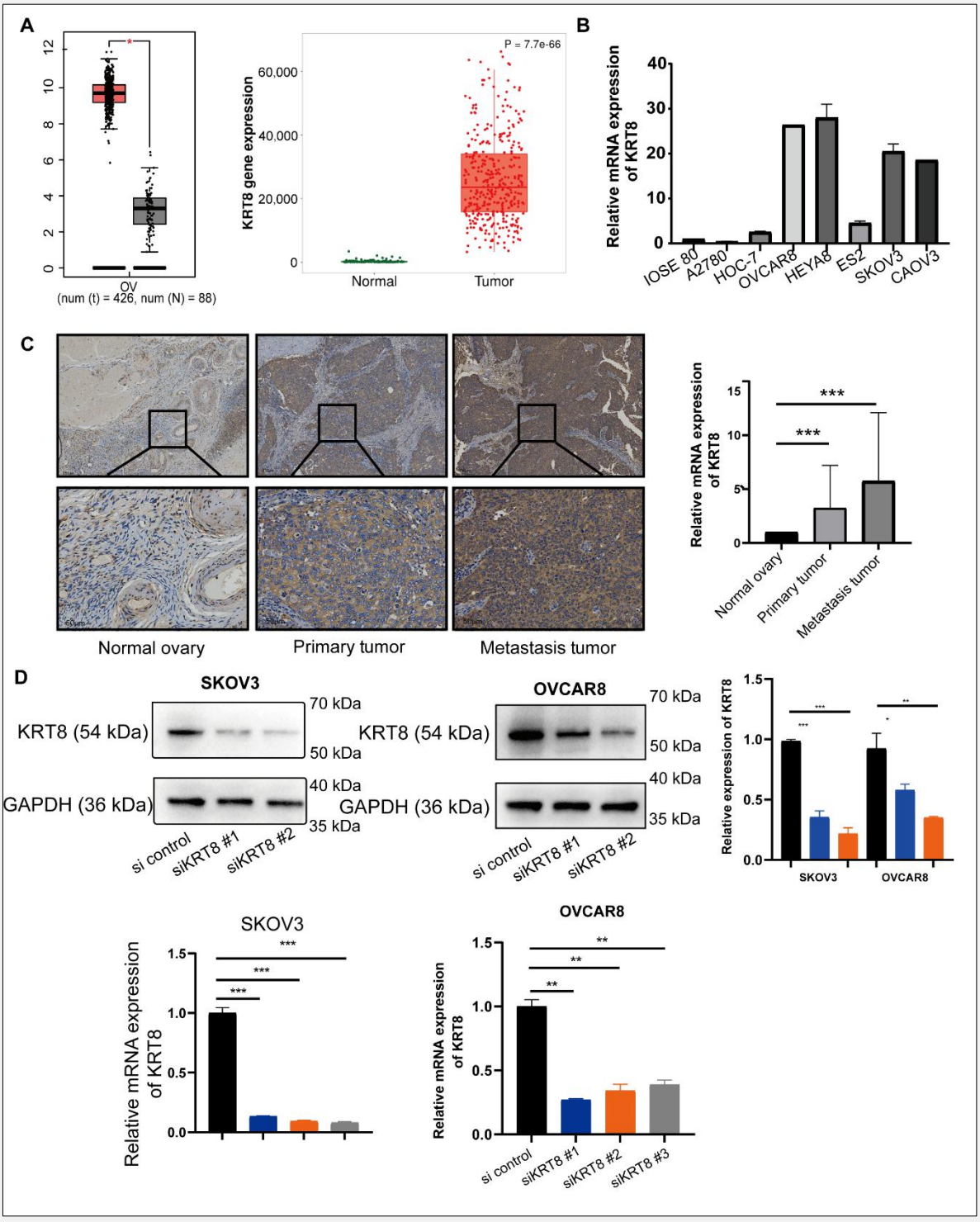

Figure 5. The expression of KRT8 in OC cell lines and tissues and verification of its overexpression and knockdown in UCEC cell lines.

A - Boxplot of KRT8 expression in normal and ovarian cancer tissues from TCGA. B - KRT8 mRNA expression in IOSE 80 and OV cell lines, including OVCAR8, HOC-7, ES2, A2780, CAOV3, and SKOV3. C - The expression of KRT8 in clinical samples (including normal ovary tissue, n = 5, primary tumor, n = 5, and metastatic tumor, n = 5). Immunohistochemistry (IHC) stain of KRT8 in clinical samples. D - Detection of the relative silencing levels of KRT8 in OVCAR8 and SKOV3 cells by qPCR. The transfection efficiency of KRT8 siRNA was determined by Western blot, obtained by ImageJ software. Data shown represent the mean ± SD (* - $p < 0.001$, ** - $p < 0.01$, * - $p < 0.05$).**

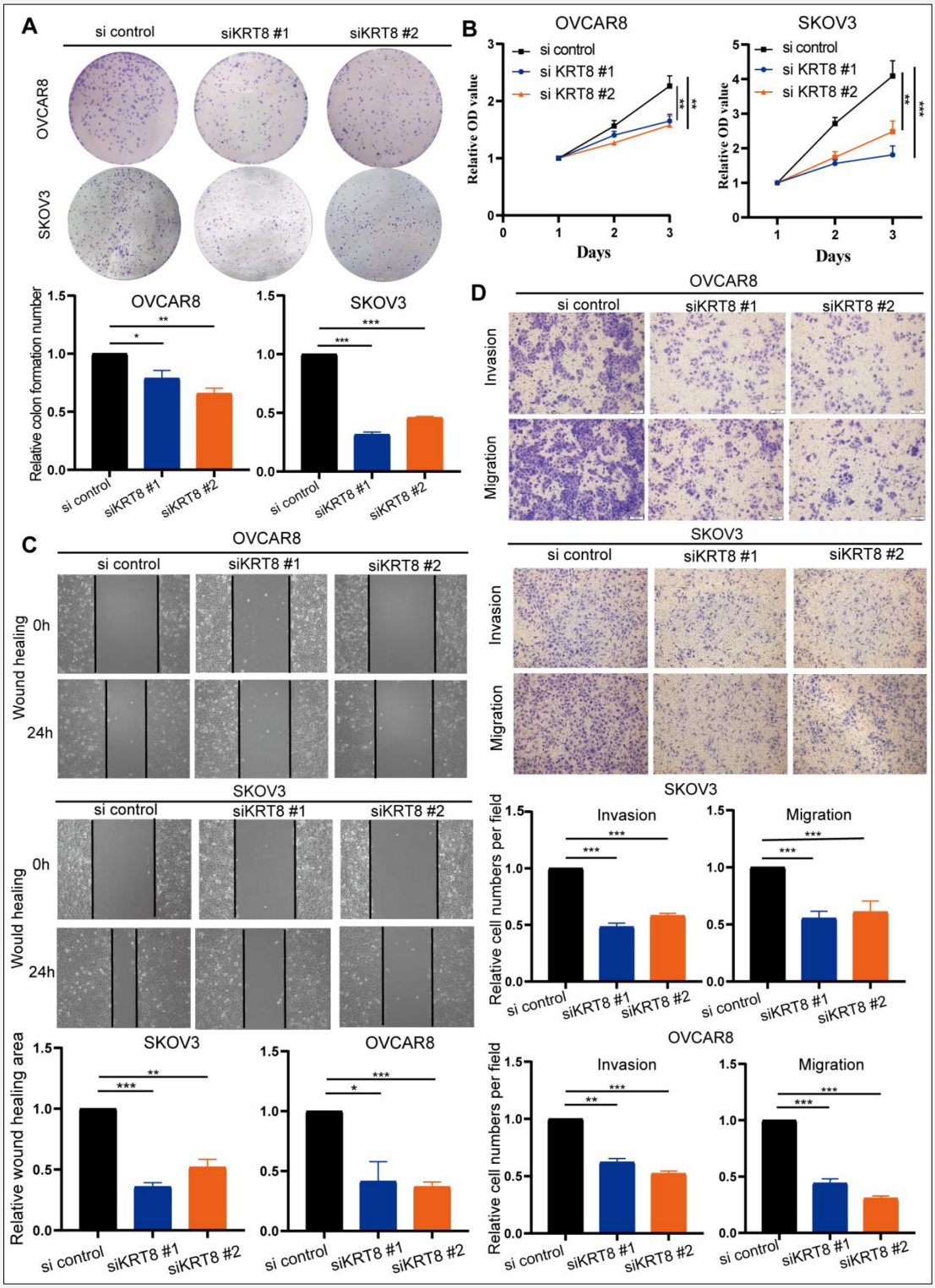

Figure 6. The biological function of KRT8 in OC cells.

A - Colon formation assays between control and KRT8 knockdown in SKOV3 and OVCAR8 cells. B - CCK8 assays were used to assess the effect of KRT8 knockdown on cell proliferation in SKOV3 and OVCAR8 cells. C - Wound healing assay in si-KRT8 and control cells. The wound healing process was monitored for 24 hours and observed under microscopy. D - Invasion and migration assays in si-KRT8 and control cells. Data shown represent the mean ± SD (* - $p < 0.001$, ** - $p < 0.01$, * - $p < 0.05$).**

vival probabilities in terms of the 1-, 2-, and 3-year survival of ovarian cancer patients (Figure 3D). These results indicated that the ERRS constructed using the TCGA dataset is an independent and significant prognostic model for predicting cancer progression and instructing clinical decisions.

Immune landscape differences between the high- and low-risk score groups of OC patients

ER stress perturbs protein-folding homeostasis in immune cells and orchestrates diverse immunomodulatory mechanisms that induce immunosuppression [14]. Previous studies report that ERS and IRE1α-XBP1 arm in T cells regulate anti-tumor function of standard treatments and current immunotherapies. In addition, XBP1 upregulation decreased intratumoral T cells infiltration by isolating from human OC cells [15]. In the analysis of the associations between ERRS and clinical factors, the immunophenotype was significantly different ($p < 0.01$) from that of the other subtypes. However, the ability of the ER stress risk score model to evaluate the immune microenvironment needs to be further investigated. Here, we estimated the difference in immune cell infiltration between the high- and low-risk score groups by CIBERSORT. A summary of the results for OC patients from the TCGA database is shown in a boxplot (Figure 4A). These results showed that immune cells exhibited significantly different infiltration between the high- and low-risk score groups and that ER stress was an impactive factor in the TIME. Next, we further examined the expression of immune checkpoint molecules in the low- and high-risk score groups. The expression levels of seven genes (PVR, CEACAM1, CD276, BTM2A1, CD274, and IDO1) were significantly lower in the high-risk group than in the low-risk group (Figure 4A). Thus, OC patients with high ER stress risk scores may have an immunosuppressive TME.

To validate the ability of the ERRS to predict treatment efficacy, we performed Kaplan-Meier and ROC analyses of the external dataset GSE140082. As shown in Figure 4B-D, patients with high-risk scores had a lower survival probability than those with low-risk scores. Although risk scores between two groups treated with bevacizumab and standard had no statistic difference, the AUC value of ERRS of 1-, 2-, and 3-year were 0.6201, 0.591, and 0.6529, which showed a significant predictive value in OC patients.

Verification of KRT8 expression in tissues and cells

KRT8 was more highly expressed in ovarian cancer tissues according to the TCGA and GTEx mRNA data (Figure 5A). Next, the mRNA and protein expression of KRT8 in normal ovarian IOSE cells and ovarian cancer cells (A2780, HOC-7, SKOV3, OVCAR8, ES2, OV CAR3, HEYA8, and CAOV3) was assessed (Figure 5B). KRT8 expression in cancer cells was greater than that in normal ovarian cells ($p < 0.05$). The increase in KRT8 expression in human ovarian cancer tissues, including 10 pairs of ovarian cancer tumor tissues and normal tissues, was further validated by IHC analysis (Figure 5C). The expression of KRT8 was examined in 5 pairs of OC and epithelial normal ovary tissues by q-PCR. Our results indicated that KRT8 was predominantly observed in the cytoplasm of OC cells and was more strongly stained than KRT8 in normal ovarian epithelium tissues (Figure 5). KRT8 mRNA expression in primary tissues was 7.55 times greater than that in normal ovarian epithelium, and in metastatic tissues, it was 10.76 times greater (Figure 5C).

KRT8 promotes ovarian cancer development

In Figure 5, the KRT8 mRNA levels in SKOV3 and OVCAR8 cells were 164 and 2.64 times greater, respectively, than those in IOSE80 cells. To further investigate the function of KRT8 in EOC, we examined the effects of KRT8 silencing in the OVCAR8 and SKOV3 cell lines using KRT8 siRNA (si-KRT8) and a negative control (si-NC). Compared with those in the si-NC group, the KRT8 mRNA in SKOV3 and OVCAR8 cells was strongly suppressed; the KRT8 mRNA level was reduced by 90% in SKOV3 cells and by 91% in OVCAR8 cells ($p < 0.05$). The KRT8 protein level decreased after 48 hours of transfection (Figure 5D). The number and volume of colonies formed by the two cell lines decreased after KRT8 gene knockdown (Figure 6A). CCK8 assays indicated that inhibition of KRT8 might markedly increase the proliferation of OC cells (Figure 6B). Next, healing and transwell experiments showed that KRT8 knockdown decreased the migration and invasion ability of OC cells (Figure 6C - D). These results indicated that KRT8 promotes malignant progression in OC *in vitro*.

DISCUSSION

OC is an aggressive disease associated with extremely poor survival. ER stress has been demonstrated to govern multiple pro-tumoral attributes in the cancer cell while dynamically reprogramming the function of innate and adaptive immune cells. Constitutively active ER stress responses enable malignant cell adaptation to oncogenic and environmental challenges while orchestrating diverse immunomodulatory mechanisms that promote malignant progression. Recent studies have uncovered that ER stress responses further impede the development of protective anti-cancer immunity by manipulating the function of myeloid cells in the tumor microenvironment. Specifically, ER stress has been shown to promote the release and cell surface translocation of calreticulin - a key damage-associated molecular pattern that facilitates immunogenic cell death (ICD) and enhances anti-tumor immune responses[16]. These studies showed that ERS is closely related to drug resistance in OC.

Various factors in the tumor microenvironment induce or block apoptosis in ovarian cancer cells through endoplasmic reticulum stress (ERS). Low glucose and met-

formin can trigger the activation of the ASK1-JNK signaling pathway related to ERS, thereby promoting cell apoptosis [17]. Changes in the expression of multiple genes in tumors regulate the sensitivity of tumor cells to chemotherapy drugs by activating downstream ERS signaling pathways. Coactivator-associated arginine methyltransferase 1 (CARM1) amplification is found in 20% of high-grade serous ovarian cancer (HGSOC). HGSOC expressing CARM1 is highly sensitive to the inhibition of IRE1α/XBP1s, and inhibiting this ER stress downstream pathway can enhance the anti-cancer effects of immune checkpoint inhibitors. The use of ER stress inhibitors to block the IRE1α/XBP1s pathway, either alone or in combination with immune checkpoint inhibitors, is a promising treatment strategy for ovarian cancer with overexpression of CARM1. The expression level of CARM1 is expected to serve as a biomarker to predict the therapeutic effect of IRE1α/XBP1s inhibitors in ovarian cancer [18]. Moreover, SWI/SNF component ARID1A is mutated in over 50% of ovarian clear cell carcinoma (OCCC). Studies have shown that ARID1A transcriptionally represses the ER stress response IRE1α-XBP1 axis, and OCCC with ARID1A mutations are sensitive to the inhibition of the IRE1α-XBP1 pathway. The activation of ARID1A is associated with the response to IRE1α-XBP1 pathway inhibition. These studies define the IRE1α-XBP1 axis of ER stress response as a target vulnerability in ARID1A-mutant OCCC, revealing a promising therapeutic approach for treating ovarian cancer with ARID1A mutations. The angiotensin II receptor type 1 (AGTR1) is involved in peritoneal metastasis of epithelial ovarian cancer (EOC), and its expression is negatively correlated with the prognosis of EOC. Activation of AGTR1 through SCD1-induced lipid desaturation weakens ER stress in cells. Cancer therapies such as radiation, chemotherapy, and targeted therapies can induce ER stress in cells, affecting their sensitivity to treatment. ERS may regulate autophagy through the mTOR and Beclin-1 pathways, leading to reduced sensitivity of SKOV3 cells to cisplatin. ER stress in tumor cells could be a potential target for improving chemotherapy efficacy and reducing tumor resistance [19]. Doxorubicin-induced ERS regulates the calcium mesh protein on the surface of ovarian cancer cells, releasing "eat me" signals to activate antitumor adaptive immunity. ER stress is involved in regulating anti-tumor immune responses in ovarian cancer. In ovarian cancer samples with elevated XBP1 expression, T cell infiltration is reduced. Additionally, the mRNA expression of interferon gamma (IFNγ), which participates in immune responses, is also lower in these patients. Advanced ovarian cancer patients often have large amounts of ascites, which suppresses T cell glucose uptake, thereby activating the IRE1α-XBP1 pathway. The activation of this pathway can inhibit mitochondrial activity and IFNγ production. Mechanistically, XBP1 can reduce the abundance of glutamine transporters, limiting the influx of glutamine in T cells under glucose deprivation conditions. Glutamine is essential for mitochondrial respiration, and inhibiting the activation of the IRE1α-XBP1 pathway can reverse this phenomenon and promote mitochondrial respiration in T cells from ascitic fluid. Therefore, ovarian cancer mice lacking XBP1 in T cells show stronger anti-tumor immunity. Controlling ER stress or targeting IRE1α-XBP1 signaling may enhance the metabolic adaptability and anti-tumor ability of T cells in cancer patients [15]. Moreover, the tumor suppressor candidate 3 (TUSC3) gene, which is located in the endoplasmic reticulum, is deleted in epithelial tumors, triggering ER stress and inducing epithelial-to-mesenchymal transition features in OC cells. Previous studies have shown that XBP1, a component of the unfolded protein response (UPR) signaling pathway, is upregulated in OC cell lines [20]. Silencing XBP1 significantly inhibits cell proliferation and enhances the sensitivity of OC cells to oxidative stress by increasing intracellular ROS levels. Inhibition of the IRE1α/XBP1s branch, either alone or combined with immune checkpoint blockade, offers a treatment strategy for various cancer types, including OC, with coactivation of coactivator-associated factor-related CARM1 overexpression. Additionally, inhibition of the IRE1α/XBP1 pathway alone or in combination with histone deacetylase 6 (HDAC6) inhibitors is an urgently needed therapeutic strategy for ARID1A-mutant OC [21]. Therefore, targeting UPR components or regulating ER stress by manipulating factors associated with ERS signaling is a promising research direction for ovarian cancer treatment.

Key findings

In this study, we present two principal findings. Firstly, a new ovarian cancer prognosis model based on endoplasmic reticulum stress gene set was introduced. Secondly, we have confirmed the expression of key genes from the model in ovarian cancer patients and cell lines and evaluated their effects on ovarian cancer cell function *in vitro*.

Strengths and limitations

This study developed a prognostic model based on a gene set associated with endoplasmic reticulum stress, utilizing six differentially expressed gene clusters to predict survival in ovarian cancer patients. Our multimetric ROC curve analysis revealed that this risk model (AUC = 0.641) outperforms age (AUC = 0.568), grade (AUC = 0.517), lymphatic invasion (AUC = 0.500), and staging (AUC = 0.528), highlighting its innovative nature. Additionally, we found that KRT8 is overexpressed in ovarian cancer, and its downregulation in in vitro cell lines suppresses proliferation and migration, offering promising biomarkers for early detection and novel therapeutic targets.

However, there remain several limitations in our research. Firstly, the ERRS should be further validated in a large database to promote clinical application. Although we found KRT8 is related to ovarian cancer, underlying mechanisms still need further investigation.

The clinical sample size should be increased to enhance the validity of the study. Furthermore, the impact of KRT8 on EMT can be further investigated to determine whether it promotes the progression of ovarian cancer and whether overexpression of KRT8 is involved in mediating ovarian cancer's response to platinum-based drugs.

Comparison with similar research

In recent years, the rapid advancement of artificial intelligence has significantly enhanced the use of neural network-based machine learning techniques for predicting cancer heterogeneity and molecular features. Various prognostic models have been developed, focusing on aspects such as ovarian cancer metastasis to the omentum, autophagy, and ferroptosis. Despite their potential, these models have limitations, including suboptimal performance on external datasets and a lack of foundational and clinical validation [22]. Additionally, the integration of single-cell sequencing data with machine learning has led to the development of sophisticated prognostic models that accurately predict the heterogeneity of the ovarian cancer tumor microenvironment [22]. Previous studies have identified endoplasmic reticulum (ER) stress as a novel characteristic of the tumor microenvironment. This stress triggers the activation of various downstream signaling proteins and leads to the accumulation of misfolded proteins, offering promising opportunities for non-invasive early diagnosis and prognostic evaluation of cancer. For instance, Chen et al. established an ER stress-related risk model for pancreatic cancer, which assists in guiding clinical decisions for immunotherapy and predicting patient survival rates [10]. However, no ER stress-related prognostic models have yet been developed for ovarian cancer. Our study addresses this critical gap.

Explanation of findings

In the present study, we identified 32 ER stress-related DEGs between normal and tumor tissues by differential expression analysis and univariate Cox analysis. Next, seven ER stress-related genes were used to construct a prognostic risk model via the LASSO repression model, which can reflect the TIME and prognostic characteristics of ovarian cancer patients and has a favorable ability to predict the prognosis of ovarian cancer patients in the GEO cohort. According to the risk scores, patients in the validation cohort were assigned to high-risk or low-risk groups. The results showed that patients in the high-risk score groups usually had a poor prognosis. In addition, when combined with clinical factors (age, stage, histologic grade, and lymphatic invasion), we confirmed that the risk score was a dependent prognostic factor. A nomogram based on clinical factors was subsequently constructed to predict survival probability and tumor progression in OC patients. The calibration curve and receiver operating characteristic (ROC) curve showed that the predicted results from the nomogram were in good agreement with the actual results, which indicates that the nomogram can be used to guide clinical practice.

KRT8, a type II basic intermediate filament (IF) protein, is the key component of cytoskeleton and involved in many cellular processes, including mitosis, differentiation, and apoptosis [23]. KRT8 expression has been found to be upregulated in obvious cancers, and its high expression can promote the cell progression and metastasis of cancer cells [24]. Genomic and transcriptomic analysis of > 5,000 patients demonstrated that KRT8 mutation and copy number amplification are frequently evident in epithelial-derived cancers. Previous studies showed that KRT8 expression is closely correlated with advanced T stage, N stage, and pathologic stage in lung adenocarcinoma (LUAD) [25]. KRT8/KRT18 ratio is a novel biomarker to predict recurrence in hepatocellular carcinoma patients [26]. These studies indicate that elevated KRT8 expression has potential to be a diagnostic and prognostic cancer biomarker in epithelial cancers. KRT8 is more than a biomarker and structural cytoskeletal protein. KRT8 protein binds to annexin A2, a protein known to mediate apoptosis as well as the redox pathway [27]. Loss of keratin 8/18 can regulate oncogenic potential by controlling various signaling pathways, including TMS1-NF-κB signaling and MARCKS L1-Paxillin1-Rac axis, in skin squamous cell carcinomas (SCC) [28]. EMT is a biologic phenomenon that can alter the state of cells along a phenotypic spectrum and cause transcriptional rewiring to produce distinct tumor cell subpopulations [29]. In lung cancer, the high expression of KRT8 regulates cell migration, invasion, and EMT by NF-kB signaling, contributing to cancer progression [25]. Cisplatin can upregulate KRT8 expression and modulate mesenchymal status of CAFs to inhibit lung cancer cell metastasis [30]. A previous study found that KRT5 mRNA expression was consistently higher in chemotherapy-resistant OC cells [31]. These results suggest that KRT8 may also be involved in mediating the response of OC cells to cisplatin.

Although KRT8 has been studied in obvious malignancies, the expression and possible role of KRT8 in OC remain unknown. In our study, the hazard ratio of KRT8 is more than 1, indicating KRT8 is a risk gene for tumor. KRT8 mRNA and protein levels were higher in OC tissues than in normal tissues. In addition, the knock-down of KRT8 by siRNA inhibited proliferation and migration of human ovarian cancer cells. These results indicated that KRT8 may exert its function by modulating cell migration and invasion in OC.

Implications and actions needed

This study employed machine learning algorithms to develop a prognostic model for ovarian cancer based on endoplasmic reticulum stress, addressing some of the challenges in diagnosing and predicting outcomes for this cancer type. This model offers valuable insights for diagnosis and prognosis. Future research should focus on validating its efficacy with extensive clinical data, further exploring the role of ER stress and key genes in

ovarian cancer progression. Single-cell technologies enable detailed cell classification and comparison, uncovering information missed in traditional tissue-level sequencing and providing more accurate and comprehensive insights. Meanwhile, spatial transcriptomics can address the loss of spatial context in single-cell studies, revealing temporal and spatial dynamics during development or tumor formation. Combining single-cell spatial data with advanced AI algorithms holds promise for becoming a crucial tool in future medical diagnostics.

CONCLUSION

In summary, endoplasmic reticulum stress-related risk signature was validated to have excellent power when used to predict survival and therapy response of ovarian cancer. Furthermore, a comprehensive analysis was conducted to explore the significant relationships between endoplasmic reticulum stress patterns and the tumor immune microenvironment, including immune cell infiltration and the expression of immune checkpoint genes. Our findings identified KRT8 expression in OV metastasis as higher than in primary tumor. KRT8 participated in ovarian cancer metastasis and presents as a potential therapeutic target for highly-malignant OV.

Acknowledgment:
We would like to thank Bai-rong Xia (The First Affiliated Hospital of USTC, Division of Life Sciences and Medicine, University of Science and Technology of China, Anhui Provincial Cancer Hospital) for the advice and useful comments that helped in finalizing this article.

Source of Funds:
This work was supported by the Clinical Key Specialty Fund of Anhui Province (no. 7507512022silczdzk), USTC Research Funds of the Double First-Class Initiative (YD9110002049), Beijing Kanghua Traditional Chinese Medicine and the Western Medicine Development Foundation (no. KH-2021-LOJJ-008), National Natural Science Foundation of China (grant number: 81872430), China Postdoctoral Science Foundation (nos. 2019T120281 and 2019M661304), and Heilongjiang Province Postdoctoral Science Foundation (no. LBH-Z18109).

Ethical Approval Statement:
Informed consent was obtained from all individual participants included in this study.

Data Availability Statement:
All data generated or analyzed during this study are included in this published article.

Declaration of Interest:
The authors declare no conflicts of interest.

References:

1. Siegel RL, Miller KD, Wagle NS, Jemal A. Cancer statistics, 2023. CA A Cancer J Clin 2023;73(1):17-48. (PMID: 36633525)
2. Schoutrop E, Moyano-Galceran L, Lheureux S, et al. Molecular, cellular and systemic aspects of epithelial ovarian cancer and its tumor microenvironment. Semin Cancer Biol 2022;86(Pt 3):207-23. (PMID: 35395389)
3. Zamarin D, Burger RA, Sill MW, et al. Randomized Phase II Trial of Nivolumab Versus Nivolumab and Ipilimumab for Recurrent or Persistent Ovarian Cancer: An NRG Oncology Study. J Clin Oncol 2020;38(16):1814-23. (PMID: 32275468)
4. Kandalaft LE, Dangaj Laniti D, Coukos G. Immunobiology of high-grade serous ovarian cancer: lessons for clinical translation. Nat Rev Cancer 2022;22(11):640-56. (PMID: 36109621)
5. Hetz C, Zhang K, Kaufman RJ. Mechanisms, regulation and functions of the unfolded protein response. Nat Rev Mol Cell Biol 2020;21(8):421-38. (PMID: 32457508)
6. Chen X, Cubillos-Ruiz JR. Endoplasmic reticulum stress signals in the tumour and its microenvironment. Nat Rev Cancer 2021; 21(2):71-88. (PMID: 33214692)
7. Cubillos-Ruiz JR, Bettigole SE, Glimcher LH. Tumorigenic and Immunosuppressive Effects of Endoplasmic Reticulum Stress in Cancer. Cell 2017;168(4):692-706. (PMID: 28187289)
8. Li G-N, Zhao X-J, Wang Z, et al. Elaiophylin triggers paraptosis and preferentially kills ovarian cancer drug-resistant cells by inducing MAPK hyperactivation. Signal Transduct Target Ther 2022;7(1):317. (PMID: 36097006)
9. Samanta S, Tamura S, Dubeau L, et al. Clinicopathological significance of endoplasmic reticulum stress proteins in ovarian carcinoma. Sci Rep 2020;10(1):2160. (PMID: 32034256)
10. Chen H, Xu N, Xu J, et al. A risk signature based on endoplasmic reticulum stress-associated genes predicts prognosis and immunity in pancreatic cancer. Front Mol Biosci 2023;10:1298077. (PMID: 38106991)
11. Hu F-F, Liu C-J, Liu L-L, Zhang Q, Guo A-Y. Expression profile of immune checkpoint genes and their roles in predicting immunotherapy response. Briefings Bioinform 2021;22(3):bbaa176. (PMID: 32814346)
12. Wain LV, Armour JAL, Tobin MD. Genomic copy number variation, human health, and disease. Lancet 2009;374(9686):340-50. (PMID: 19535135)
13. Macintyre G, Goranova TE, De Silva D, et al. Copy number signatures and mutational processes in ovarian carcinoma. Nat Genet 2018;50(9):1262-70. (PMID: 30104763)
14. Wang X, Hu R, Song Z, et al. Sorafenib combined with STAT3 knockdown triggers ER stress-induced HCC apoptosis and cGAS-STING-mediated anti-tumor immunity. Cancer Lett 2022; 547:215880. (PMID: 35981569)
15. Song M, Sandoval TA, Chae C-S, et al. IRE1α–XBP1 controls T cell function in ovarian cancer by regulating mitochondrial activity. Nature 2018;562(7727):423-8. (PMID: 30305738)

16. Abdullah TM, Whatmore J, Bremer E, Slibinskas R, Michalak M, Eggleton P. Endoplasmic reticulum stress-induced release and binding of calreticulin from human ovarian cancer cells. Cancer Immunol Immunother 2022;71(7):1655-69. (PMID: 34800147)

17. Ma L, Wei J, Wan J, et al. Low glucose and metformin-induced apoptosis of human ovarian cancer cells is connected to ASK1 via mitochondrial and endoplasmic reticulum stress-associated pathways. J Exp Clin Cancer Res 2019;38(1):77. (PMID: 30760281)

18. Lin J, Liu H, Fukumoto T, et al. Targeting the IRE1α/XBP1s pathway suppresses CARM1-expressing ovarian cancer. Nat Commun 2021;12(1):5321. (PMID: 34493732)

19. Tian J, Liu R, Qu Q. Role of endoplasmic reticulum stress on cisplatin resistance in ovarian carcinoma. Oncol Lett 2017;13(3): 1437-43. (PMID: 28454274)

20. Kratochvílová K, Horak P, Ešner M, et al. Tumor suppressor candidate 3 (TUSC3) prevents the epithelial-to-mesenchymal transition and inhibits tumor growth by modulating the endoplasmic reticulum stress response in ovarian cancer cells. Int J Cancer 2015;137(6):1330-40. (PMID: 25735931)

21. Duska LR, Zamarin D, Hamilton E, et al. Phase IIa Study of PLX2853 in Gynecologic Cancers With Known ARID1A Mutation and Phase Ib/IIa Study of PLX2853/Carboplatin in Platinum-Resistant Epithelial Ovarian Cancer. JCO Precis Oncol 2023;7: e2300235. (PMID: 37797273)

22. Zhang D, Lu W, Cui S, Mei H, Wu X, Zhuo Z. Establishment of an ovarian cancer omentum metastasis-related prognostic model by integrated analysis of scRNA-seq and bulk RNA-seq. J Ovarian Res 2022;15(1):123. (PMID: 36424614)

23. Hesse M, Zimek A, Weber K, Magin TM. Comprehensive analysis of keratin gene clusters in humans and rodents. Eur J Cell Biol 2004;83(1):19-26. (PMID: 15085952)

24. Xie L, Dang Y, Guo J, et al. High KRT8 Expression Independently Predicts Poor Prognosis for Lung Adenocarcinoma Patients. Genes (Basel) 2019;10(1):36. (PMID: 30634629)

25. Chen H, Chen X, Pan B, Zheng C, Hong L, Han W. KRT8 Serves as a Novel Biomarker for LUAD and Promotes Metastasis and EMT via NF-κB Signaling. Front Oncol 2022;12:875146. (PMID: 35664775)

26. Golob-Schwarzl N, Bettermann K, Mehta AK, et al. High Keratin 8/18 Ratio Predicts Aggressive Hepatocellular Cancer Phenotype. Transl Oncol 2019;12(2):256-68. (PMID: 30439626)

27. Guo D, Xu Q, Pabla S, et al. Cytokeratin-8 in Anaplastic Thyroid Carcinoma: More Than a Simple Structural Cytoskeletal Protein. Int J Mol Sci 2018;19(2):577. (PMID: 29443941)

28. Fortier A-M, Asselin E, Cadrin M. Keratin 8 and 18 Loss in Epithelial Cancer Cells Increases Collective Cell Migration and Cisplatin Sensitivity through Claudin1 Up-regulation. J Biol Chem 2013;288(16):11555-71. (PMID: 23449973)

29. Padhye A, Konen JM, Rodriguez BL, et al. Targeting CDK4 overcomes EMT-mediated tumor heterogeneity and therapeutic resistance in KRAS-mutant lung cancer. JCI Insight 2021;6(17): e148392. (PMID: 34309585)

30. Li X, Song Q, Guo X, et al. The Metastasis Potential Promoting Capacity of Cancer-Associated Fibroblasts Was Attenuated by Cisplatin via Modulating KRT8. Onco Targets Ther 2020;13: 2711-23. (PMID: 32280245)

31. Ricciardelli C, Lokman NA, Pyragius CE, et al. Keratin 5 overexpression is associated with serous ovarian cancer recurrence and chemotherapy resistance. Oncotarget 2017;8(11):17819-32. (PMID: 28147318)

32. Chen J, Hong JH, Huang Y, et al. EZH2 mediated metabolic rewiring promotes tumor growth independently of histone methyltransferase activity in ovarian cancer. Mol Cancer 2023;22(1):85. (PMID: 37210576)

33. Jones BA, Varambally S, Arend RC. Histone Methyltransferase EZH2: A Therapeutic Target for Ovarian Cancer. Mol Cancer Ther 2018;17(3):591-602. (PMID: 29726819)

34. Trisdale SK, Schwab NM, Hou X, Davis JS, Townson DH. Molecular manipulation of keratin 8/18 intermediate filaments: modulators of FAS-mediated death signaling in human ovarian granulosa tumor cells. J Ovarian Res 2016;9(1):8. (PMID: 26911253)

35. Chacón C, Mounieres C, Ampuero S, Urzúa U. Transcriptomic Analysis of the Aged Nulliparous Mouse Ovary Suggests a Stress State That Promotes Pro-Inflammatory Lipid Signaling and Epithelial Cell Enrichment. Int J Mol Sci 2023;25(1):513. (PMID: 38203684)

36. Wang S, Wang C, Li X, et al. Down-regulation of TRIB3 inhibits the progression of ovarian cancer via MEK/ERK signaling pathway. Cancer Cell Int 2020;20(1):418. (PMID: 32874132)

Additional material can be found online at:
http://supplementary.clin-lab-publications.com/241216/